Solar wind structure suggested by bimodal correlations of solar wind speed and density between the spacecraft SOHO and Wind

K. W. Ogilvie,[1] M. A. Coplan,[2] D. A. Roberts,[1] and F. Ipavich[2]

Received 1 January 2007; revised 30 March 2007; accepted 7 May 2007; published 15 August 2007.

[1] We calculate the cross-spacecraft maximum lagged-cross-correlation coefficients for 2-hour intervals of solar wind speed and density measurements made by the plasma instruments on the Solar and Heliospheric Observatory (SOHO) and Wind spacecraft over the period from 1996, the minimum of solar cycle 23, through the end of 2005. During this period, SOHO was located at L1, about 200 R_E upstream from the Earth, while Wind spent most of the time in the interplanetary medium at distances of more than 100 R_E from the Earth. Yearly histograms of the maximum, time-lagged correlation coefficients for both the speed and density are bimodal in shape, suggesting the existence of two distinct solar wind regimes. The larger correlation coefficients we suggest are due to structured solar wind, including discontinuities and shocks, while the smaller are likely due to Alfvénic turbulence. While further work will be required to firmly establish the physical nature of the two populations, the results of the analysis are consistent with a solar wind that consists of turbulence from quiet regions of the Sun interspersed with highly filamentary structures largely convected from regions in the inner solar corona. The bimodal appearance of the distributions is less evident in the solar wind speed than in the density correlations, consistent with the observation that the filamentary structures are convected with nearly constant speed by the time they reach 1 AU. We also find that at solar minimum the fits for the density correlations have smaller high-correlation components than at solar maximum. We interpret this as due to the presence of more relatively uniform Alfvénic regions at solar minimum than at solar maximum.

Citation: Ogilvie, K. W., M. A. Coplan, D. A. Roberts, and F. Ipavich (2007), Solar wind structure suggested by bimodal correlations of solar wind speed and density between the spacecraft SOHO and Wind, *J. Geophys. Res.*, *112*, A08104, doi:10.1029/2007JA012248.

1. Introduction

[2] Multispacecraft observations are required to understand many aspects of the solar wind flow. Correlations between various quantities measured by different spacecraft provide insights into the correlation lengths in the flow [e.g., *Collier et al.*, 1998] and the orientation of "fronts" that can consist of shocks, discontinuities, or general wave fields [e.g., *Richardson and Paularena*, 1998; *Weimer et al.*, 2003]. Here we correlate Solar and Heliospheric Observatory (SOHO) and Wind observations of speed and density upstream of the Earth to further elucidate the solar wind structure.

[3] The multispacecraft study of correlations between solar wind properties in the interplanetary medium has been pursued for both space science and space weather related purposes using plasma and magnetic field observations upstream of the Earth [*Crooker et al.*, 1982; *Russell et al.*, 1983; *Couzens and King*, 1986; *Collier et al.*, 1998; *King and Papitashvili*, 2005; *Richardson et al.*, 1998; *Richardson and Paularena*, 1998, 2001; *Weimer et al.*, 2003]. These studies have produced useful results concerning transverse and radial correlation scales and anisotropies of wave front distributions in the solar wind. In particular, these studies have established that there is a wide distribution of normals to the "fronts" (correlated structures between spacecraft) with a peak in the direction of the normals between the radial and the Parker spiral field angle [e.g., *Richardson and Paularena*, 1998]. Such multispacecraft studies are important for determining the proper lag between single spacecraft measurements and the encounter of interplanetary structures with the Earth's magnetosphere [see *Bargatze et al.*, 2005, and references therein].

[4] Here we continue and extend work previously reported by *Coplan et al.* [2001] who used data at two resolutions to determine that distribution of front normals for the mass flux was, on average, in the same quadrant as the average Parker spiral, consistent with previous results for other quantities. This study also included some three spacecraft correlations that indicated the normals to the fronts were, on average, inclined to the ecliptic by some tens of degrees. Here we focus on a different set of questions, using a larger data set that covers much of the

[1]Heliospheric Science Division, NASA Goddard Space Flight Center, Greenbelt, Maryland, USA.
[2]Department of Physics, University of Maryland, College Park, Maryland, USA.

Copyright 2007 by the American Geophysical Union.
0148-0227/07/2007JA012248

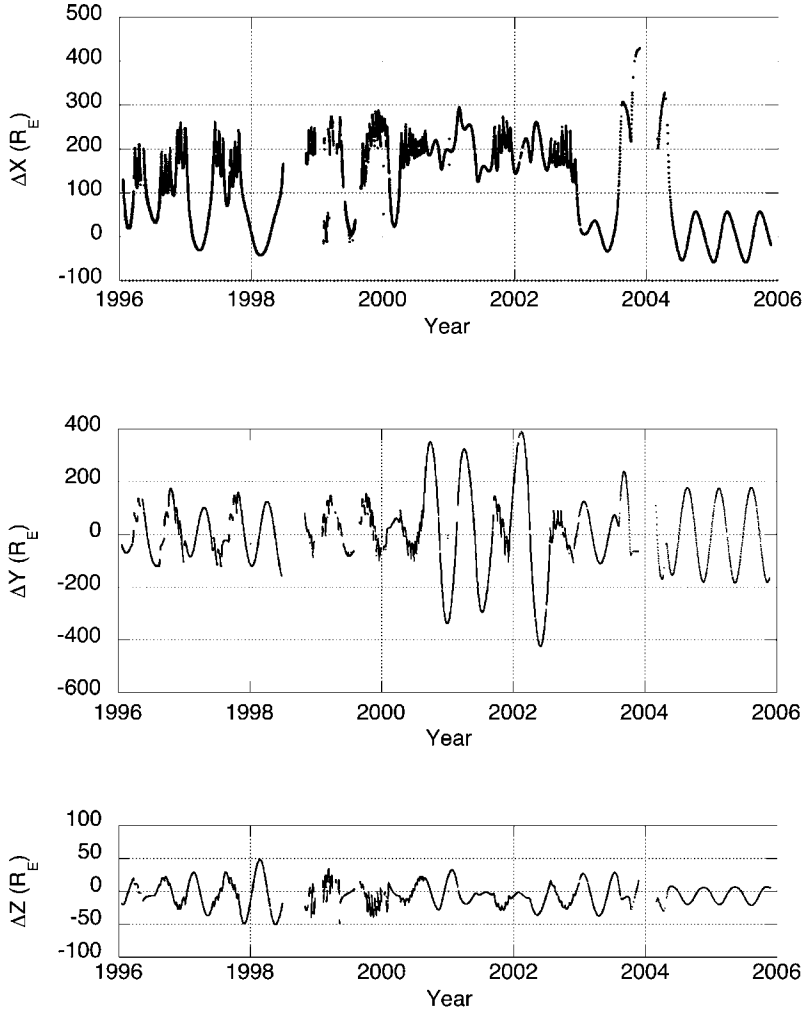

Figure 1. Interspacecraft distances, (Solar and Heliospheric Observatory-Wind), (ΔX, ΔY, ΔZ), for the period 1996 through 2002.

solar activity cycle. Of particular interest is the examination of the distributions of maximum correlations between time series from two spacecraft for the speed and density of the plasma. This examination lends support to the picture of a "two-component" solar wind in which structured regions with sharp magnetic rotations and strong density striations are distinguished from more uniform regions of what is commonly termed Alfvénic turbulence. The idea of structures (often termed "spaghetti-like") in the solar wind dates back at least to the work of *McCraken and Ness* [1966]; these ideas will be discussed more fully in a later section.

[5] In the next two sections we discuss the spacecraft trajectories and data analysis. We then present the main results on the interspacecraft correlations and offer an interpretation of these results in terms of the solar wind picture mentioned above, which is briefly compared to other "two-component" solar wind models. The final section summarizes and discusses the results.

2. Spacecraft Trajectories

[6] The SOHO spacecraft, launched in 1995, is situated in a halo orbit (31 $\times$ 102 R_E semiaxes), with a period of 180 days, around the L1 point approximately 200 R_E upstream from Earth in the solar wind [*Domingo et al.*, 1995]. The Wind spacecraft [*Russell*, 1995], launched in 1994, has occupied various positions in the solar wind including ones at distances 300 to 400 R_E in the positive and negative Y_{GSE} directions. Our data are derived from the Mass Time-of-Flight (MTOF) plasma instrument on SOHO and the Solar Wine Experiment (SWE) instrument on Wind. Both instruments are well calibrated, have been cross-calibrated, and have been remarkably stable since launch [*Kasper et al.*, 2005].

[7] The coordinate system used is a Geocentric Solar Ecliptic system (GSE) with its origin at the Earth. The X-axis is directed toward the Sun, so that angles in the X–Y plane are measured from the X axis in the counterclockwise direction as viewed from above the Z = 0 plane. The orbits of the two spacecraft are such that the separations between them in the X and Y directions are typically an order of magnitude greater than in the Z direction. The differences (SOHO position – Wind position) between the spacecraft positions (ΔX, ΔY, ΔZ) are shown as functions of time in Figure 1, which covers the years 1996 through 2005. The figure shows that ΔX varied between 126 R_E and 330 R_E

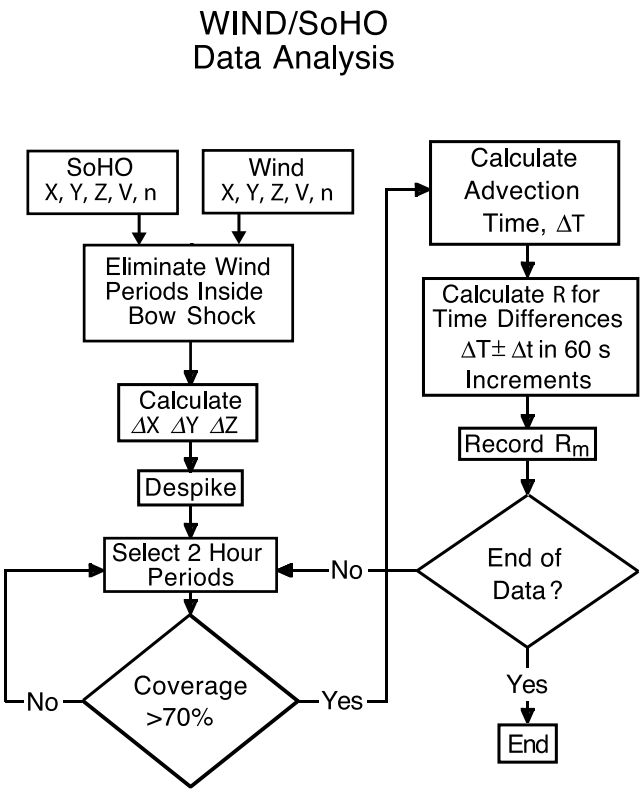

Figure 2. Block diagram of the analysis scheme. The calculation of the correlation coefficients is carried out using MatLab routines.

during the whole of 2001, while ΔZ varied between $\pm 31\ R_E$ and ΔY changed from 314 R_E to $-330\ R_E$ as Wind passed from one side of the Earth-Sun line to the other. During this time, SOHO also traversed the Earth-Sun line but with much smaller excursions.

3. Data Analysis

[8] The method of analysis of the plasma measurements used in this paper is very similar to that described by *Coplan et al.* [2001] but will be briefly described here for convenience. The basic SOHO data are taken at 30 s sampling intervals, and those from Wind are taken at 96 s sampling intervals. The solar wind plasma observations from the instruments on the two spacecraft are adjusted to a 96-s cadence based on the Wind measurements by linearly interpolating SOHO points either side of each Wind point. Our previous experience tells us that the results shown here would not change if, for example, bin averages were used to reconcile the resolutions. Figure 2 shows a simplified block diagram of the analysis procedure. Files, represented by boxes at the top of the chart, contain equally spaced time series for speed, density, and flux from SOHO and Wind, and for the magnetic field from Wind in the form of 2-hour averages. After the relative positions of the spacecraft have been calculated, impulsive noise ("spikes") is eliminated from the data using an algorithm by *Roberts* [1993] in which a running 5-sigma criterion based on 100-point intervals is used to successively eliminate spurious points.

[9] For the calculation of correlations, 2-hour intervals of data are used. The correlation coefficient that is used is the standard linear correlation coefficient, r, also called Pearson's r. It is given by the formula

$$r = \frac{\sum_i (x_i - \bar{x})(y_i - \bar{y})}{\sqrt{\sum_i (x_i - \bar{x})^2}\sqrt{\sum_i (y_i - \bar{y})^2}} \tag{1}$$

where the overbar indicates the mean of the corresponding quantity. Here, the values of x refer to one spacecraft, and y to the other, and the two time series are shifted with respect to each other to find r as a function of the lag, using the overlapping points in the correlation.

[10] There are sufficient individual data points (75 for the 2-hour interval using the 96 s cadence) for meaningful correlations to be calculated; we estimate the error in the correlation to be on the order of the bin size we use for the analysis below, i.e., less than 0.03. The distance traveled by the solar wind during a 2-hour interval ($\sim$400 R_E) is greater than the radial separation between the spacecraft. Only periods when data from both instruments in the solar wind are available for at least 70% of the time are selected. The average spacecraft separation ΔX and the average solar wind speed V_{SW} over the interval determine a radial convection propagation time between the spacecraft, ΔT. Cross-correlation coefficients are calculated between SOHO data and Wind data shifted in time by $\Delta T \pm \Delta t$, where Δt is changed by 60 s increments to 3600 s. For each 2-hour period the maximum correlation is recorded from the 120 calculated correlation coefficients, so that during a year $365 \times 12 = 4380$ maximum correlation coefficients can be obtained. Henceforth we will refer to the maximum, lagged correlation coefficient (i.e., the maximum of the cross-correlation function) as simply the "correlation coefficient," denoted R_m.

[11] The lag for the highest correlation has been used in many studies, but here we focus on the correlation coefficients themselves. *Coplan et al.* [2001, Figure 3] plotted two examples of high- and low-speed wind time series and the corresponding cross-correlation functions for plasma flux at SOHO and Wind, measured during the year 1997. The correlation coefficient, R_m, was 0.97 in the better-correlated case and 0.38 in the less-well correlated case. The high correlation was clearly the consequence of strong, rapid variations in solar wind speed and density, while the low correlation came from more uniform flow. It has been well known since at least the work of *Belcher and Davis* [1971] that Alfvénic intervals do not show such variations in density and flow speed. Here, similar calculations are done for every year in 2-hour intervals.

[12] Table 1 summarizes the data sets and some overview information about them, the entry labeled "Days of Observation" is calculated by dividing the total number of 2-hour observations in each year by 12. We note that there are 2 years, 1998 and 2001, during which the number of 2-hour periods was rather low. We will examine the yearly distributions of speed and density correlations to determine their shape and how it varies over the solar activity cycle between the years 1996 and 2005. In Table 1, the

Table 1. Statistics for the Years 1996 to 2005[a]

Year	1996	1997	1998	1999	2000	2001	2002	2003	2004	2005
Sunspot numbers	9	22	64	93	120	111	104	64	40	30
Shocks[b]	9	36	44	60	82	87	70	-	-	-
R_m (Speed)	0.54	0.52	0.50	0.49	0.51	0.50	0.47	0.52	0.53	0.55
R_m (Density)	0.54	0.54	0.50	0.50	0.53	0.54	0.51	0.49	0.50	0.52
Days of observation	306	260	202	251	324	213	303	294	281	305
Number of observations	3669	3123	2419	3010	3891	2554	3632	3527	3373	3662

[a]$N_1 + N_2$ = total number of correlations, N_2 = number of correlations from the higher Gaussian fit. Sunspot numbers from World Data Center for the Sunspot Index, Royal Observatory of Belgium.
[b]D. Berdichevsky (private communication, 2004).

number of 2-hour observation periods and the sunspot number are given for the years 1996 through 2005.

4. Distributions of Correlation Coefficients

[13] We initially noticed that the distributions of correlation coefficients of density for all years are noticeably bimodal so we have fitted all of the data with both a single Gaussian and the sum of two Gaussian functions to examine this point more closely. The equations for the unimodal and bimodal Gaussians are

$$N(m) = m_1 \exp\left\{-(m_2 - m)^2/m_3\right\} \tag{2}$$

and

$$N(m) = m_1 \exp\left\{-(m_2 - m)^2/m_3\right\} + m_4 \exp\left\{-(m_5 - m)^2/m_6\right\} \tag{3}$$

that is, we fit the distribution for the number of correlations in bin m, $N(m)$, with one or two Gaussians with independent means (m_2 and m_5), amplitudes (m_1 and m_4), and variances (m_3 and m_6). Both standard and weighted least squares fits were used, with no qualitative differences; here we report the weighted case.

[14] We have calculated a weighted χ^2 for all fits based on the equation

$$\chi^2 = \Sigma(N(m) - N_m)^2/N(m) \tag{4}$$

where N_m is the measured number of points in bin m and the sum is over values of m. We have ignored contributions with $N(m)$ less than 10 to limit the contribution of statistically poorly determined points. The denominator is the statistical measure of square the standard deviation in the measurement, so a value of $\chi^2 \sim 27$ (the number of bins) implies that the fit is within one standard deviation of the measurements, on average.

[15] To illustrate another way in which one clear type of structured region contributes to large correlations, Figure 3 shows a histogram of the correlation coefficients obtained during 130 periods in 2000 and 2001 identified by *Berdichevsky et al.* [2000] and in subsequent work (D. Berdichevsky, private communication, 2004) as times of occurrence of shocks, which can easily be identified in the time series and yield high values of correlation coefficient for both speed and density. The distribution clearly contributes to the high correlation peak of the distributions. Shocks will contribute to a greater extent to the distributions at solar maximum, as indicated by the occurrences in Table 1, although they are not dominant at any time in the solar cycle.

[16] The results of the fitting procedure are shown in Figures 4 and 5 that show distributions and fits for each year. In Figure 4 the distribution of correlation coefficients for speed is shown along with single- and double-Gaussian fits. In this case, the two fits are usually quite similar. In contrast, Figure 5 shows the double-Gaussian fit and the two underlying Gaussians; in this case bimodal distributions are essential for good fits, and the two lighter curves show the relative importance of the two types of distributions. We note that the 27 points are represented very well using six parameters. These empirical fits are representations rather than explanations of the distributions, but they provide a quantitative description, and because of the random nature of the fluctuations and the random occurrence of discontinuities, the representation has plausibility. Also, their quality suggests that the bimodality may have a physical cause and does not, for example, result from statistical fluctuations.

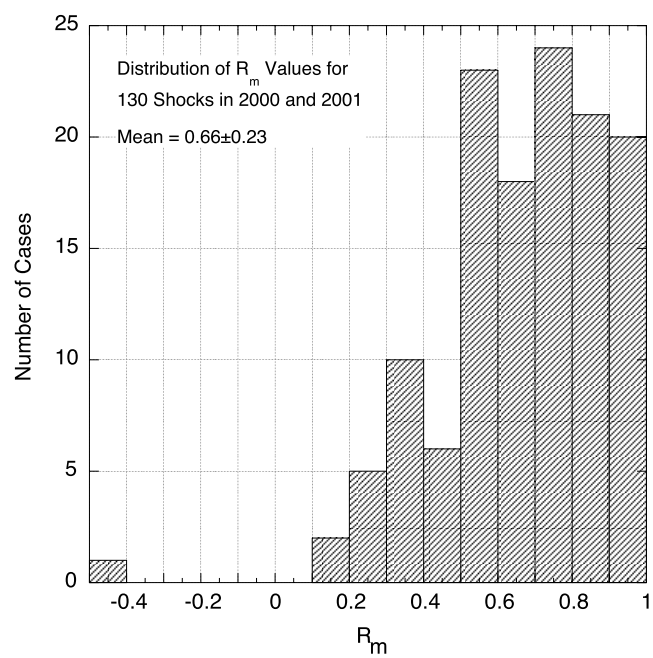

Figure 3. A histogram of correlation coefficients of density during 130 periods in 2000 and 2001 when shocks were observed (D. Berdichevsky, private communication, 2004).

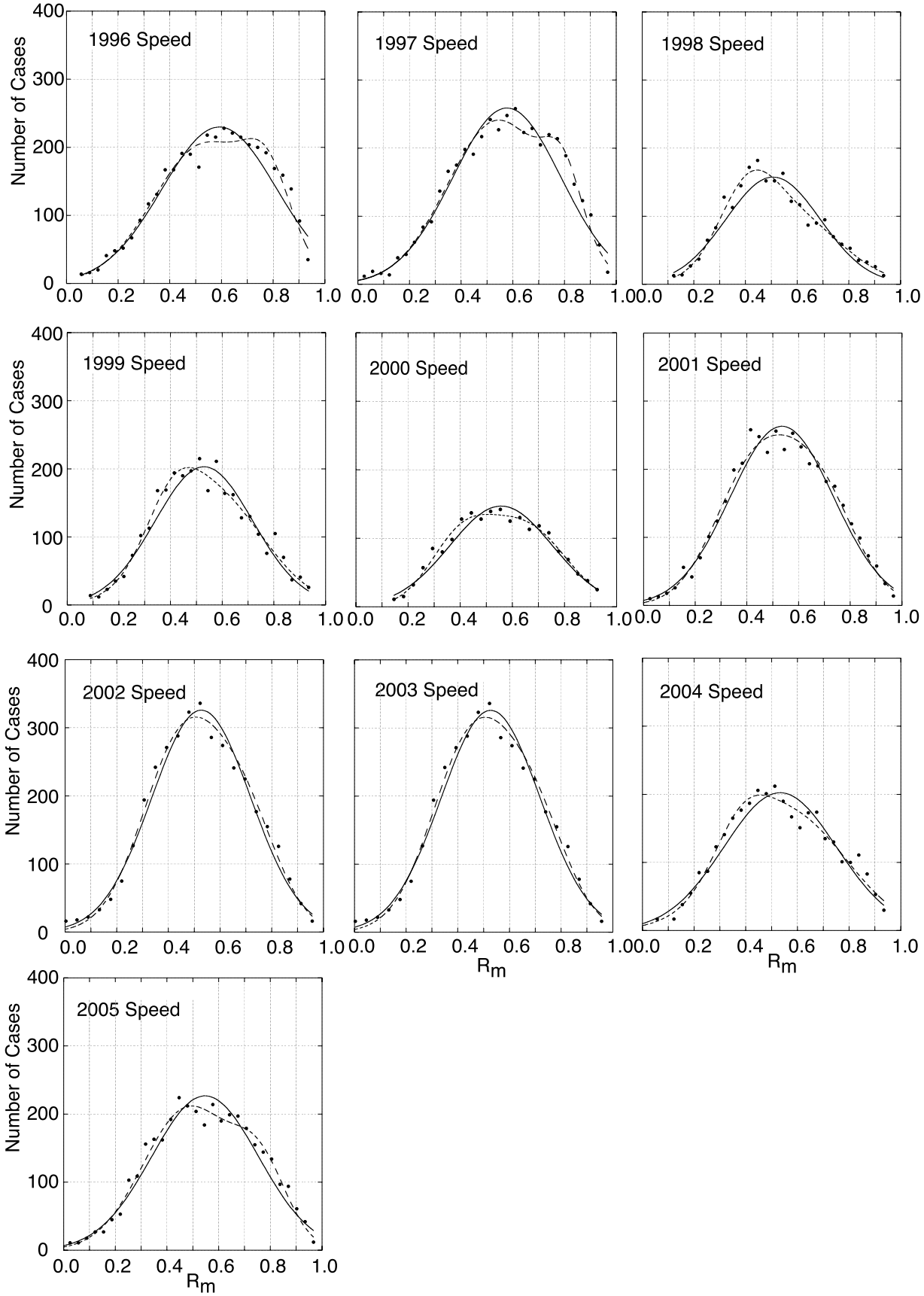

Figure 4. Histograms of correlation coefficients of speed for all the years of this study with the two Gaussian distributions of the unimodal and bimodal fits are shown for each case.

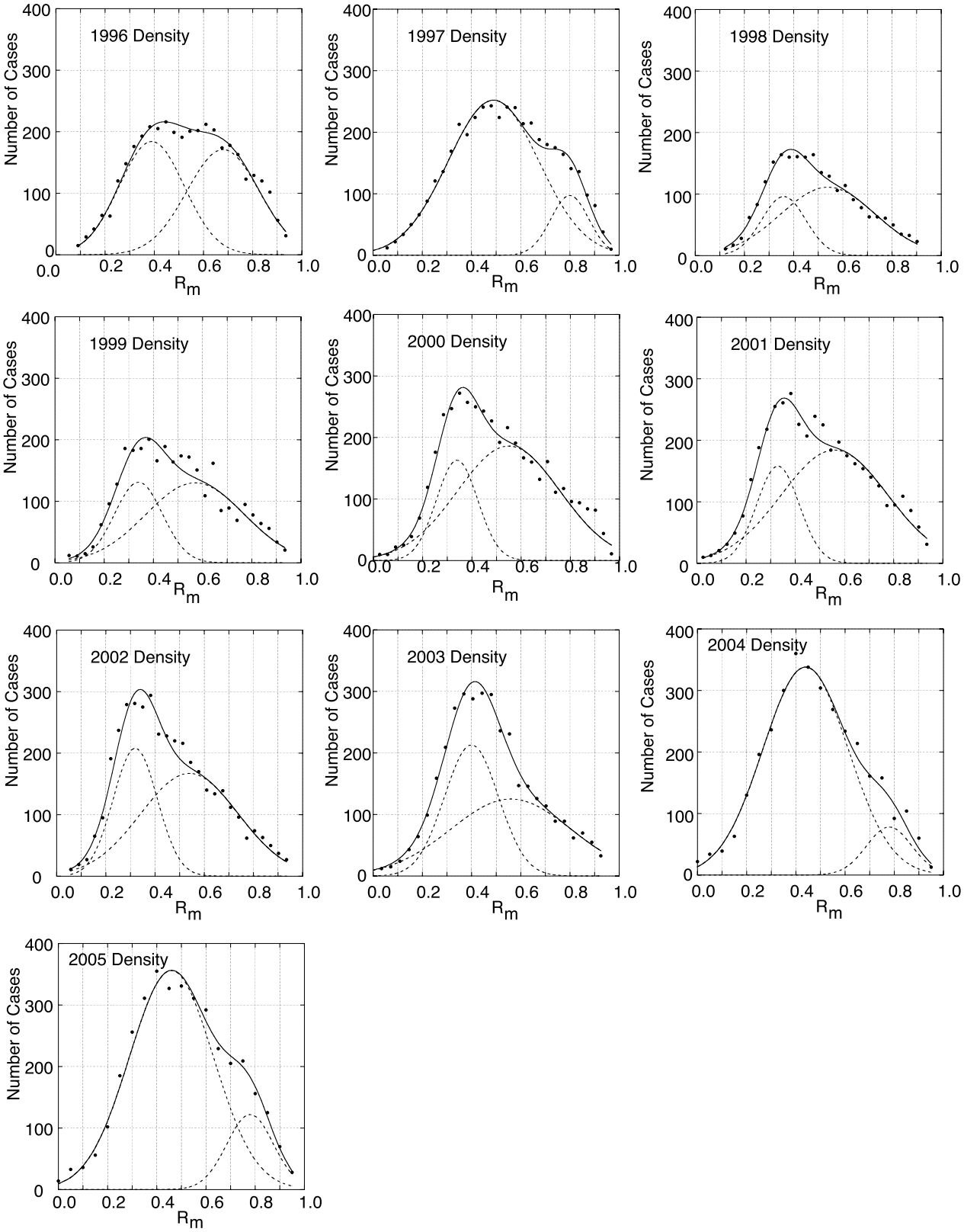

Figure 5. Similar to Figure 4, but for density data. Here the bimodal fits and the two component Gaussian curves are shown.

Table 2a. Yearly Fit Parameters and χ^2 for Speed Correlations[a]

	Single Gaussian		Double Gaussian			
Year	m_1	χ^2	m_1	m_4	χ^2	χ^2 Ratio
1996	230 ± 5	80	205 ± .7	99 ± 16	34	0.4
1997	259 ± 5	123	241 ± 8	94 ± 19	52	0.4
1998	157 ± 4	75	91 ± 12	101 ± 12	22	0.3
1999	203 + /5	66	164 ± 5	68 ± 8	35	0.5
2000	147 ± 4	31	88 ± 4	116 ± 7	11	0.7
2001	263 ± 5	56	193 ± 7	159 ± 5	39	0.6
2002	326 ± 7	48	137 ± 10	284 ± 10	34	0.7
2003	232 ± 5	111	81 ± 10	192 ± 6	63	0.6
2004	202 ± 5	77	60 ± 5	172 ± 9	46	0.6
2005	227 ± 5	90	209 ± 8	100 ± 19	42	0.5

[a]The first three columns refer to single Gaussian fits, the next three refer to double Gaussian fit, and the last column is the ratio between χ^2 for double to single Gaussian. The numbers are rounded to integers. Note that values of χ^2 are smallest around solar maximum. For speed the single Gaussian typically produces nearly as good a fit as the double Gaussian.

Table 3a. Bimodal Fit Parameters for the Distributions of Speed Correlations[a]

Year	m_1	m_2	m_3	m_4	m_5	m_6	$(m_4/m_1)\sqrt{m_6/m_3}$
1996	205.	0.537	0.0795	99.3	0.782	0.0163	0.22
1997	241.	0.544	0.0776	93.6	0.796	0.0109	0.15
1998	91.1	0.407	0.0240	101.	0.570	0.0746	1.95
1999	67.8	0.404	0.0207	164.	0.561	0.0767	4.66
2000	88.5	0.398	0.0288	116.	0.651	0.0493	1.71
2001	193.	0.427	0.0470	158.	0.676	0.0427	0.78
2002	284.	0.460	0.05	137.	0.704	0.0342	0.40
2003	81.4	0.380	0.0170	192.	0.544	0.0780	5.05
2004	59.7	0.380	0.0209	172.	0.564	0.1	6.30
2005	209.	0.484	0.0612	99.6	0.765	0.0215	0.28

[a]The last column represents the relative number of occurrences in the high-correlation set compared to the low-correlation set, as determined by the area under each Gaussian.

[17] In Tables 2a and 2b we present statistics from the whole set of speed and density readings for 1996 to 2005. The ratio column in the tables shows (χ^2 double Gaussian)/(χ^2 single Gaussian). The double Gaussian is a better fit to the points in each case than the single Gaussian as a result of having more degrees of freedom, but the improvement is most striking for the double Gaussian fit to the density. The ratios in the last column of the table, as well as the graphs in Figures 4 and 5, show that the speed is in many cases well-represented by the single Gaussian fit, whereas the density is almost always much better represented by a double Gaussian.

[18] We note that there is a solar cycle effect, especially in the density correlations. The presence of highly structured winds due to the lack of large coronal holes at solar maximum will naturally lead to a greater presence of the second peak in the distribution of density correlations. This is shown most prominently in the last column of Table 3b, which gives the ratio of the number of events in the high-correlation set to those in the low-correlation set. At solar minimum, this ratio is much less than unity (~0.2), whereas at the height of the solar cycle in 2000–2001, this ratio approaches 3. Also, the smallest χ^2 ratio in Table 2b is for the density in 2001, the year with the second highest sunspot number, and other maximum years of 2000 and 2002 are also poorly fit by single Gaussians. The structures in the speed, in the meantime, are not correlated with solar cycle, as shown in Table 3a, which is expected from the scenario discussed in the next section.

5. A Possible Interpretation

[19] The state of the solar wind is conventionally characterized as "fast" or "slow," but other divisions are possible. Recent work on planar magnetic structures (PMSs) [*Roberts et al.*, 2004] suggests a division into two states roughly described as "structured" and "turbulent." In the former, strong field rotations that produce a minimum magnetic field variance perpendicular to the mean field are accompanied by density striations and a low correlation of velocity and magnetic field fluctuations (the Alfvénicity). PMSs are extreme examples of this state. The turbulent regime typically has less abrupt and more random rotations, high Alfvénicity, and very small density variations. This characterization of the wind corresponds to some extent to the speed characterization, with the slow wind being typically more structured, but there are good examples of slow flow that are Alfvénic and in many respects like "typical" fast flows [e.g., *Marsch et al.*, 1981; *Roberts et al.*, 1987].

[20] The idea of structured regions in the solar wind flow has been discussed since shortly after the discovery of the wind itself, starting with the work of *McCraken and Ness* [1966] who used the idea of flux tubes to explain properties of energetic particle propagation. *Mariani et al.* [1973] found evidence that discontinuities in the interplanetary medium are often associated with spaghetti-like tubes rather

Table 2b. Same as Table 2a, but for Density

	Single Gaussian		Double Gaussian			
Year	m_1	χ^2	m_1	m_4	χ^2	χ^2 Ratio
1996	228 ± 5	93	184	171	30	0.32
1997	258 ± 5	117	252 ± 6	95 ± 12	31	0.26
1998	156 ± 4	125	96	111 ± 7	19	0.15
1999	186 ± 5	228	131 ± 10	130 ± 7	72	0.32
2000	244 + /5	309	163 ± 10	186 ± 7	76	0.25
2001	242 ± 5	253	158 ± 11	184 ± 9	37	0.15
2002	239 ± 5	217	208 ± 11	167 ± 7	42	0.19
2003	270 ± 6	215	213 ± 15	125 ± 14	40	0.19
2004	324 + /7	91	338 ± 18	78 ± 16	51	0.56
2005	347 ± 7	86	356 ± /12	122 ± 12	27	0.31

Table 3b. Same as Table 3a, but for Density

Year	m_1	m_2	m_3	m_4	m_5	m_6	$(m_4/m_1)\sqrt{m_6/m_3}$
1996	184.	0.387	0.0350	171.	0.685	0.0430	1.03
1997	251.	0.490	0.0686	96.9	0.797	0.0124	0.16
1998	96.4	0.363	0.0156	111.	0.543	0.0742	2.51
1999	131.	0.340	0.0187	130.	0.572	0.0801	2.05
2000	163.	0.336	0.0140	186.	0.555	0.0874	2.85
2001	158.	0.329	0.0151	184.	0.560	0.0931	2.89
2002	208.	0.317	0.0156	167.	0.539	0.0789	1.81
2003	212.	0.398	0.0238	125.	0.559	0.116	1.30
2004	338.	0.443	0.0605	78.3	0.781	0.0169	0.12
2005	355.	0.456	0.0586	122.	0.781	0.0179	0.19

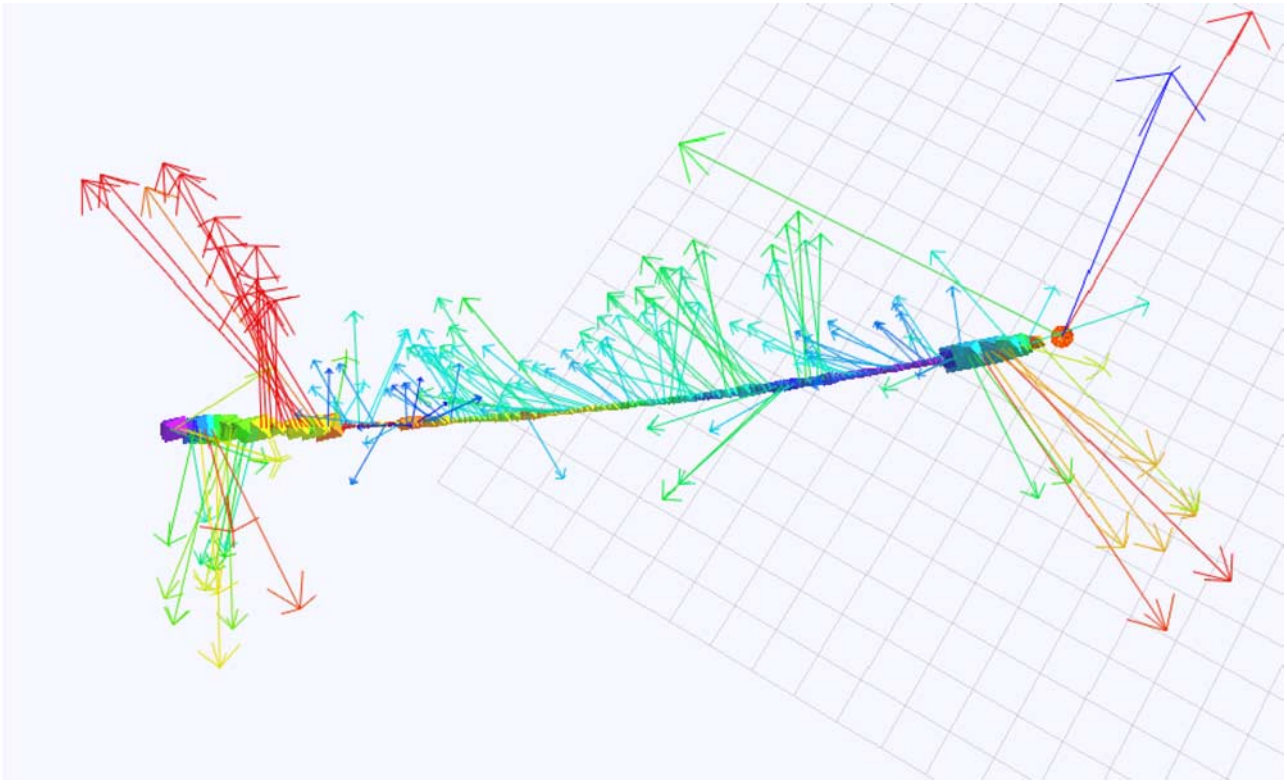

Figure 6. Hourly average data from the Omni tape displayed in a kinematic projection, showing the presence of Alfvénic turbulence in the middle of the period and rapid rotations at the ends; see text.

than the sheets depicted by *Burlaga* [1968], although in retrospect both may occur. More recently, regions of convected structures have been associated with regions that are relatively non-Alfvénic [*Bruno and Bavassano*, 1991], and, at least at times, these have relatively small velocity fluctuations ("magnetic field directional turnings" of *Tu and Marsch* [1991; see also *Tu and Marsch*, 1993]). In the present work, unlike the others sited above, we identify structures using the criterion of a density correlation signature, although it is likely that there is a significant overlap in the regions identified. In related recent work, J. King (private communication, 2007) found that density correlations similar to those found here could be separated into a bimodal distribution easily identified by low and high values of the variance of the density. While it is intuitively clear that high-density variances should be associated with high correlations, what is not obvious is that there should be two distinct classes of correlations. The speed of the wind did not correlate well with the maximum correlations. (See below for an illustration of these ideas.) It is worth noting that *Thieme et al.* [1990] identified what they suggested were flux tubes of coronal origin in Alfvénic high speed streams, and thus the true picture may be one in which the continuously variable structure of the solar atmosphere is imposed on the wind at all times, but that where there are strong striations (as in helmet streamers), the structures become dominant, and where there are not the ubiquitous waves are dominant. Clearly there is much work to be done to clarify the relationships between the various types of "structures" so far identified in the solar wind.

[21] Figure 6 shows a typical example of two types of wind envisioned here, using a kinematic projection of the hourly averaged OMNI data (http://omniweb.gsfc.nasa.gov) from 1997-04-10 1221 UT to 1997–04-17 0348 UT and assuming the rapid flow sweeps slowly changing spatial structures across the spacecraft. The method of display is described by *Roberts et al.* [2005]. The display effectively shows a spatial view of the magnetic field vectors, colored according to magnitude (0.3–13 nT, purple to red). Symbols along the axis are colored according to speed (300 to 500 km/s) and sized according to number density (3 to 45 cm^{-3}). The view is nearly from the north (blue axis); the red and green (X and Y) axes are in the ecliptic plane, and the red circle to the right represents the location of the Sun. The vectors all appear as measured at 1 AU, not scaled or evolved with a model according to distance from the Sun. The middle region is typical of Alfvénic turbulence, whereas the ends show rapid rotations similar to planar magnetic structures (PMSs) in extreme cases, such as the high field regions on the left. Typical structures appear to correspond to flux tubes, and thus density may vary strongly from one to the next, but the speed can be relatively constant as the tubes are convected beside each other (see Figure 7 which displays 96-s Wind data for part of the interval in Figure 6). In particular, the highly filamentary portions of the interval shown in Figures 6 and 7 have rapidly varying densities, with changes of a factor of 3 in within minutes, whereas the speed only varies by a few percent, with few rapid changes, over the same intervals. These structures lead naturally to large values of R_m for density and smaller

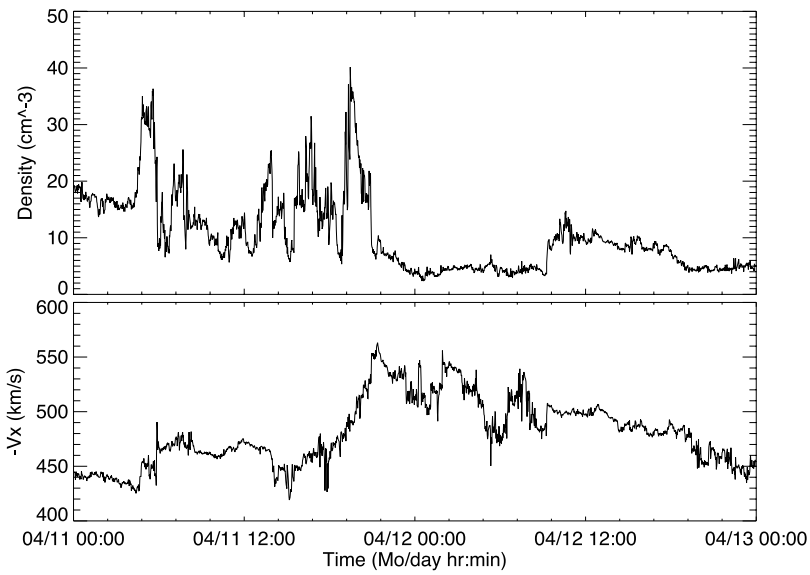

Figure 7. Time series for the (left) early part of the data in Figure 6, showing the highly structured density and relatively unstructured speed. Note that low-speed wind, seen at the two ends of the figure, can be structured or unstructured in the density. The data here are from the Wind Solar Wind Experiment instrument at 96-s resolution.

values of R_m for speed and are consistent with highly structured wind being convected fairly uniformly from the Sun. The structures will lead to strong correlations between spacecraft for sharply defined density structures, of the kind observed in the present study. Thus the two populations found here are consistent with a picture of the solar wind as consisting of generic turbulence from quiet solar regions interspersed with highly filamentary regions convected from near the solar surface. Both populations will evolve, but the filamentary structures, in this view, retain their character well past 1 AU. The regions of general turbulence do not show striking density variations, and in fact tend to have fairly constant density as originally pointed out by *Belcher and Davis* [1971]. This will lead to less pronounced interspacecraft correlations, which correspond naturally to the set of lower maximum correlations discussed above.

6. Discussion and Conclusions

[22] Using speed and density data from the stable and reliable MTOF and SWE instruments on the SOHO and Wind spacecraft, we have been able to study the correlations between plasma quantities measured at these spacecraft over the period from the minimum of solar cycle 23 to the succeeding solar maximum in 2000–2002 and on to 2005. When exhibited as histograms, we find that the distributions of correlation coefficients have maxima at approximately 0.4 to 0.55. The distribution of the calculated correlation coefficients for each year can be very well fitted by single Gaussian functions for speed and double Gaussian functions for density. The average maxima of the two Gaussians occur at 0.37 ± 0.03 and 0.67 ± .03, respectively, over the period 1996 to 2005. A proportion of the highest correlations are contributed by shocks in the solar wind, but the sharp density jumps in structured regions outnumber the shocks by a large factor. We suggest that the correlations showing a maximum at 0.37 result from turbulence in the solar wind, while the higher maximum is due to convected flux tubes and some shocks characteristic of "structured" regions. In this picture, the presence of a much stronger high-correlation component for density is due to the flux tubes of different density being convected together at comparable speeds, as shown in Figure 7. We suggest that this study provides additional evidence for a division of the solar wind into two states that are somewhat related to, but distinct from, slow and fast wind. In this view, much of what is often termed a third state of the wind, namely transient events, would fall into the structured class.

[23] Recent work [*Burlaga and Vinas*, 2004] on the structure of the magnetic field and speed at 1 AU, using observations made with the ACE spacecraft, cover a much wider range of time periods than are covered here, and indicate that a generalization of the Tsallis probability distribution function [*Tsallis et al.*, 1995, 2002] provides a multiscale description of those observations. At small timescales they emphasize the importance of shocks and discontinuities, while CIRs and other disturbances dominate the large scales. The present observations with SOHO and Wind are consistent with those of Burlaga and Viñas, but their approach indicates both a different way of dividing up the space of fluctuations and a possible way to tie our two populations together. In particular, their work suggests that we are dealing with a continuous distribution of types of fluctuations from which we are emphasizing the contrasts at the extremes. The distinctness of the distributions we find, and the implications of different sources and character of the two distributions, make this view of two classes of fluctuations useful, just as it is useful to classify high- and low-speed streams even though these, too, are part of a continuum well-described by a Tsallis distribution when considered from a purely statistical point of view.

[24] **Acknowledgments.** We thank A. Gross and D. Roy and M. Holland for assistance with the data reduction and analysis and the NSSDC for provision of the OMNI data. This research was partially supported by NASA grant NNG05GO13G.

[25] Amitava Bhattacharjee thanks the reviewers for their assistance in evaluating this paper.

References

Bargatze, L. F., R. L. McPherron, J. Minamora, and D. Weimer (2005), A new interpretation of Weimer et al.'s solar wind propagation delay technique, *J. Geophys. Res.*, *110*, A07105, doi:10.1029/2004JA010902.

Belcher, J. W., and L. Davis Jr. (1971), Large amplitude Alfven waves in the interplanetary medium, *J. Geophys. Res.*, *76*, 3534.

Berdichevsky, D. A., A. Szabo, R. P. Lepping, A. F. Vinas, and F. Mariani (2000), Interplanetary fast shocks and associated drivers observed through the twenty third solar minimum by Wind over its first 2.5 years, *J. Geophys. Res.*, *105*, 27,289.

Bruno, R., and B. Bavassano (1991), Origin of low cross-helicity regions in the inner solar wind, *J. Geophys. Res.*, *96*, 7841.

Burlaga, L. F. (1968), Microscale structure in the interplanetary medium, *Solar Phys.*, *4*, 67.

Burlaga, L. F., and A. Vinas (2004), Multiscale structure of the magnetic field and speed at 1 AU during the declining phase of solar cycle 23 described by a generalized Tsallis probability distribution function, *J. Geophys. Res.*, *109*, A12107, doi:10.1029/2004JA010763.

Collier, M. R., J. A. Slavin, R. P. Lepping, A. Szabo, and K. W. Ogilvie (1998), Timing accuracy for a simple planar propagation of magnetic structures in the solar wind, *Geophys. Res. Lett.*, *25*, 2509.

Coplan, M. A., F. Ipavich, J. King, K. W. Ogilvie, D. A. Roberts, and A. J. Lazarus (2001), Correlation of solar wind parameters between SOHO and Wind, *J. Geophys. Res.*, *106*, 18,615.

Couzens, D. A., and J. H. King (1986), Interplanetary Medium Data Book, suppl. 3, *1977–1985 NSSDC/WDC-A-R&S 86-04*, NASA Goddard Space Flight Cent., Greenbelt, Md. (Available online at http://omniweb.gsfc.nasa.gov/om_book/sup3/s3_main.html.)

Crooker, N. U., G. L. Siscoe, C. T. Russell, and E. J. Smith (1982), Factors controlling the degree of correlation between ISEE 1 and ISEE 3 interplanetary magnetic field measurements, *J. Geophys. Res.*, *87*, 2224.

Domingo, V., B. Fleck, and A. I. Poland (1995), The SOHO mission: An overview, *Solar Phys.*, *162*, 1.

Kasper, J. C., A. J. Lazarus, J. T. Steinberg, K. W. Ogilvie, and A. Szabo (2005), Physics-based tests to identify the accuracy of solar wind ion measurements: A case study with the Wind Faraday Cups, *J. Geophys. Res.*, *111*, A03105, doi:10.1029/2005JA011442.

King, J. H., and N. E. Papitashvili (2005), Solar wind spatial scales in and comparisons of hourly Wind and ACE plasma and magnetic field data, *J. Geophys. Res.*, *110*, A02104, doi:10.1029/2004JA010649.

Mariani, F., B. Bavassano, U. Villante, and N. F. Ness (1973), Variations of occurence rate of discontinuities in the interplanetary magnetic field, *J. Geophys. Res.*, *78*, 8011.

Marsch, E., H. Rosenbauer, R. Schwenn, K.-H. Muehlhaeuser, and K. U. Denskat (1981), Pronounced proton core temperature anisotropy, ion differential speed, and simultaneous Alfvén wave activity in slow solar wind at 0.3 AU, *J. Geophys. Res.*, *86*, 9199.

McCraken, K. G., and N. F. Ness (1966), Collimation of cosmic rays by interplanetary magnetic field, *J. Geophys. Res.*, *71*, 3315.

Richardson, J. D., and K. I. Paularena (1998), The orientation of plasma structure in the solar wind, *Geophys. Res. Lett.*, *25*, 2097.

Richardson, J. D., and K. I. Paularena (2001), Plasma and magnetic field correlations in the solar wind, *J. Geophys. Res.*, *106*, 239.

Richardson, J. D., F. Dasevisky, and K. I. Paularena (1998), Solar wind correlations between L1 and Earth, *J. Geophys. Res.*, *103*, 14,619.

Roberts, D. A. (1993), An algorithm for finding spurious points in turbulent signals, *Comput. Phys.*, *7*, 599.

Roberts, D. A., M. L. Goldstein, L. W. Klein, and W. H. Matthaeus (1987), Origin and evolution of fluctuations in the solar wind - Helios observations and Helios-Voyager comparisons, *J. Geophys. Res.*, *92*, 12,023.

Roberts, D. A., M. Luckyanova, V. Rezapkin, and R. Boller (2004), Insights into planar magnetic solar wind structures using new visualization methods, *Eos Trans. AGU*, *84*(47), Fall Meet. Suppl., Abstract SH21C-0432.

Roberts, D. A., P. A. Keiter, and M. L. Goldstein (2005), Origin and dynamics of the heliospheric streamer belt and current sheet, *J. Geophys. Res.*, *110*, A06102, doi:10.1029/2004JA010541.

Russell, C. T. (Ed.) (1995), *The Global Geospace Mission*, Kluwer Acad., Dordrecht, Netherlands.

Russell, C. T., M. M. Mellott, E. J. Smith, and J. H. King (1983), Multiple spacecraft observations of interplanetary shocks Four spacecraft determination of shock normals, *J. Geophys. Res.*, *88*, 4739.

Thieme, K. M., E. Marsch, and R. Schwenn (1990), Spatial structures in high-speed streams as signatures of fine-structures in coronal holes, *Ann. Geophys.*, *8*, 713.

Tsallis, C., S. V. F. Levy, A. M. C. Souza, and R. Maynard (1995), Statistical-mechanical foundation of the ubiquity of Lévy distributions in Nature, *Phys. Rev. Lett.*, *75*, 3589.

Tsallis, C., A. Rapisarda, V. Latora, and F. Baldovin (2002), Nonextensivity: From low-dimensional maps to Hamiltonian systems, in *Dynamics and Thermodynamics of Systems With Long Range Interactions*, *Lect. Not. in Phys.*, vol. 602, edited by T. Dauxois et al., pp. 140–162, Springer, New York.

Tu, C.-Y., and E. Marsch (1991), A case study of very low cross-helicity fluctuations in the solar wind, *Ann. Geophys.*, *9*, 319.

Tu, C.-Y., and E. Marsch (1993), A model of solar wind fluctuations with two components: Alfvén waves and convective structures, *J. Geophys. Res.*, *98*, 1257.

Weimer, D. R., D. M. Ober, N. C. Maynard, M. R. Collier, D. J. McComas, N. F. Ness, C. W. Smith, and J. Watermann (2003), Predicting interplanetary magnetic field (IMF) propagation delay times using the minimum variance technique, *J. Geophys. Res.*, *108*(A1), 1026, doi:10.1029/2002JA009405.

K. W. Ogilvie and D. A. Roberts, Heliospheric Science Division, NASA Goddard Space Flight Center, Greenbelt, MD 20771, USA. (aaron.roberts@nasa.gov)

M. A. Coplan and F. Ipavich, Department of Physics, University of Maryland, College Park, MD 20742, USA.